energies

MDPI

Article

Effect of the Temperature on the Magnetic and Energetic Properties of Soft Magnetic Composite Materials

Luca Ferraris [1,*], Fausto Franchini [1], Emir Pošković [1], Marco Actis Grande [2] and Róbert Bidulský [3]

[1] Department of Energy, Politecnico di Torino, Viale T. Michel 5, 15121 Alessandria, Italy; fausto.franchini@polito.it (F.F.); emir.poskovic@polito.it (E.P.)
[2] Department of Applied Science and Technology, Politecnico di Torino, Viale T. Michel 5, 15121 Alessandria, Italy; marco.actis@polito.it
[3] Agency for the Support of Regional Development Kosice, Kosice Self-Governing Region, Strojarenská 3, 04001 Kosice, Slovakia; robert.bidulsky@tuke.sk
* Correspondence: luca.ferraris@polito.it; Tel.: +39-013-122-9366

Abstract: In recent years, innovative magnetic materials have been introduced in the field of electrical machines. In the ambit of soft magnetic materials, laminated steels guarantee good robustness and high magnetic performance but, in some high-frequency applications, can be replaced by Soft Magnetic Composite (SMC) materials. SMC materials allow us to reduce the eddy currents and to design innovative 3D magnetic circuits. In general, SMCs are characterized at room temperature, but as electrical machines operate at high temperature (around 100 °C), an investigation analysis of the temperature effect has been carried out on these materials; in particular, three SMC samples with different binder percentages and process parameters have been considered for magnetic and energetic characterization.

Keywords: soft magnetic composites; magnetic device; measurement; electric machine; thermal stress; iron losses

Citation: Ferraris, L.; Franchini, F.; Pošković, E.; Actis Grande, M.; Bidulský, R. Effect of the Temperature on the Magnetic and Energetic Properties of Soft Magnetic Composite Materials. *Energies* **2021**, *14*, 4400. https://doi.org/10.3390/en14154400

Academic Editors: Javier Contreras and Luca Ferraris

Received: 25 May 2021
Accepted: 13 July 2021
Published: 21 July 2021

1. Introduction

Magnetic materials play a significant role in many applications; they are most widespread in the electrical machines sector. Recently, new magnetic materials were developed and adopted in various electrical motors, overcoming traditional solutions that begin showing several technological limits. Between the innovative materials, a significant part is occupied by the so called Soft Magnetic Composites (SMCs); generally speaking, they consist of ferromagnetic particles covered by an insulating layer [1–3]. The layer can be of organic (metal oxides) [4–16] or inorganic origin (resins) [17–27]. SMCs can successfully integrate into several applications concerning electrical machines [28–32] and power electronics (EMI filter) [33,34]. Thanks to the reduced contribution of eddy currents losses, SMCs can operate at medium-high frequencies keeping their magnetic characteristics almost unchanged [35–37]. Furthermore, such materials give the possibility to design innovative electrical motors with very complex geometries, taking advantage of their 3D behavior [28]. Between these electrical machines, axial flux motor (AFM) [38,39], transverse flux motor (TFM) [40–42], claw pole motor (CPM) [43] and others [44–46] should be cited and considered of significant interest for the operators of the sector.

Normally SMCs characterization data are provided at room temperature, but the operating temperature of electrical motors, generally at about 70–100 °C, can reach up to 150 °C, making necessary further activity for the materials characterization.

The work focuses on the investigation of the magnetic and energetic properties of these materials for the typical operating temperatures of the applications in which they should be adopted. Different SMC specimens have been tested and analyzed: the polymeric binder content and compacting pressure level have been considered as primary parameters of the study. Interesting and useful results emerged, with a view towards industrial applications.

2. Phenomenon Description and Procedure

The role of the thermal energy in helping to overcome the Barkhausen jumps is well-known in the literature [47,48]. Such an advantage is more pronounced in the first part of the magnetic characteristic, in which Barkhausen jumps play a primary role. Near the saturation zone, the magnetization process is much more reversible than irreversible, and thus the effects of the considered temperature variations are also less pronounced.

This fact influences the hysteresis cycle area and, therefore, its energy, with an immediate impact on the global efficiency value. Still, few attempts tried to quantify its influence in the typical electrical machine temperature range.

A starting point on this topic could eventually lead in the future to an increase in the rated working temperature for an electrical machine equipped with SMCs, to reach better efficiency values.

This phenomenon is less pronounced in the laminated steel, where the Barkhausen jumps are limited.

2.1. Specimen Preparation

The SMC samples used in this research study have been produced through the mixing of very pure iron powder and a polymer binder. Such binder is an epoxy resin suitable to operate in high temperature, until 200 °C and more, showing good mechanical strength. The binder content is usually under 1 wt %: in the proposed activity, two percentages in weight have been selected: 0.5 wt %. and 0.2 wt %. [28]. After the mixing process, the SMC powder was compacted through a hydraulic press. Two pressure levels are adopted in work: 400 MPa and 700 MPa [16,49]. The obtained shape is toroidal and is wound with two windings.

The specimen identification has the following coding rules: the E letter represents the epoxy resin, while the next digits correspond to the binder content in weight; the last number is the pressure level. For instance, the SMC material with 0.5% of epoxy resin, compacted at 700 MPa is identified with E 0.5-700.

2.2. Experimental Procedure

The electrical machines usually operate around 100 °C. For this reason, the prepared SMC samples have been tested at different temperatures [50]. Mainly, it was necessary to implement a particular system able to warm the samples without dispersing the heat. In this context, a special chamber was prepared with wood walls (Figure 1); inside the chamber, a thermocouple was positioned next to the SMC sample to control the temperature values. The chamber has been placed above a heater, and the temperature feedback loop involved the aforementioned thermocouple, through the heater's external TC input (Figure 2). The temperature distribution inside the chamber is reported in Figure 3, for the temperature set at 125 °C.

The magnetic characterization has been performed at the following temperature values: 20 °C, 50 °C, 75 °C, 100 °C, and 125 °C. The measurements (Figure 4) began after a suitable temperature settling time of at least 15 min, in a steady-state condition.

No air flux compensation coil was used, as stated in the standard.

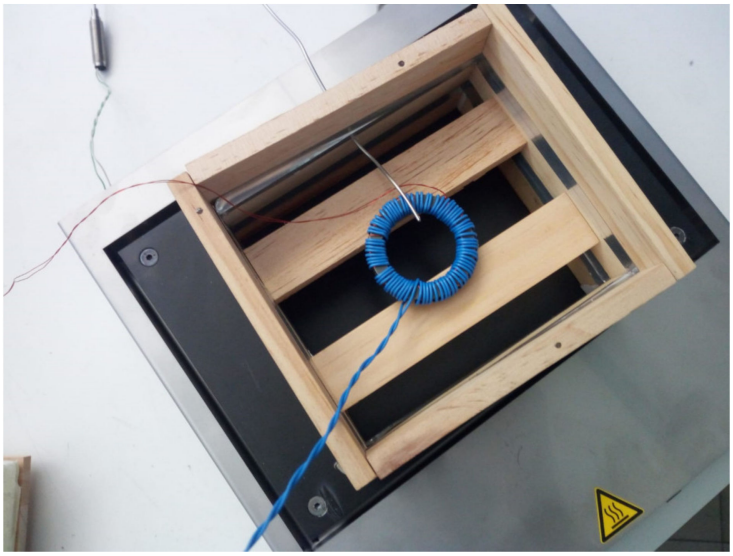

Figure 1. The toroid Soft Magnetic Composite (SMC) samples inside the implemented chamber (without cover).

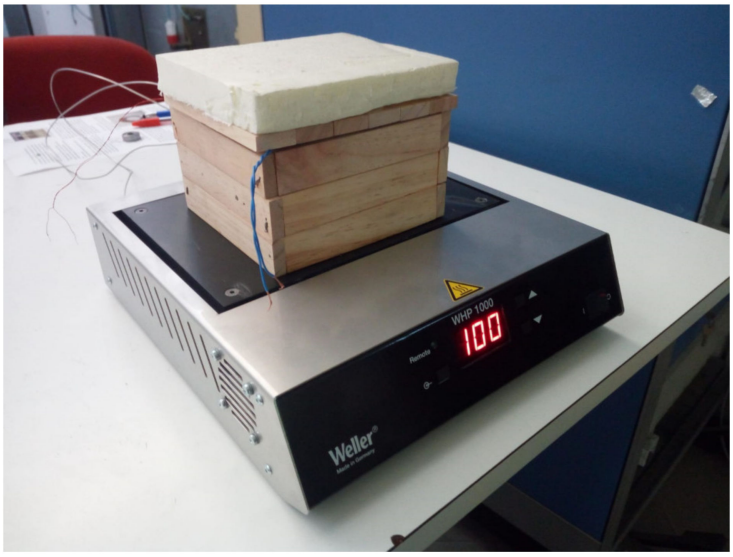

Figure 2. The heating process: chamber and heater at 100 °C.

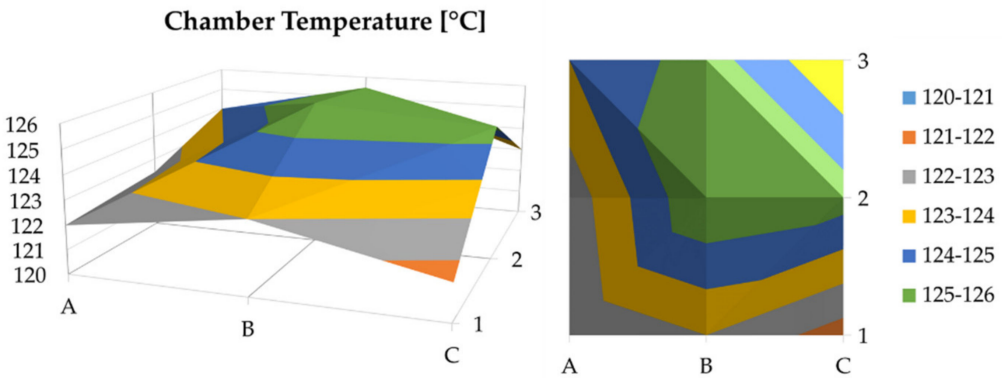

Figure 3. Temperature distribution inside the chamber with temperature set at 125 °C.

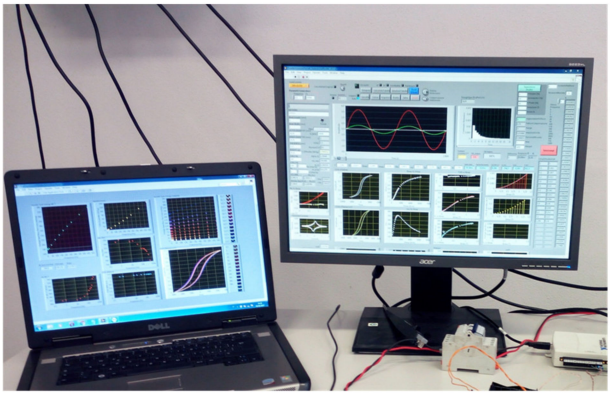

Figure 4. Interface of magnetic characterization software.

3. Experimental Results

A detailed experimental activity has been conducted on three different SMC specimens: low binder content and low compaction (E 0.2-500), low binder content and high compaction (E 0.2-700), and high binder content and high compaction (E 0.5-700). In Table 1, the main characteristics of each specimen are reported, together with the mechanical information in terms of Transverse Rupture Strength (TRS) obtained with the three points bending test.

Table 1. Specimens properties.

Specimen	Binder %	Mold Pressure (MPa)	Density (g/cm^3)	TRS @20 °C (MPa)
E 0.2-500	0.2%	500	7.02	39.5
E 0.2-700	0.2%	700	7.37	84.5
E 0.5-700	0.5%	700	7.28	120.7

TRS—Transverse Rupture Strength.

The measurement procedure followed the EN 60404-4 standard, except for the diameter ratio (external over internal), which was 1.33 in the present work, against the maximum stated of 1.25.

The magnetic and energetic characterization [51] is carried out with the so called "transformer approach", with two windings wounded around the toroidal magnetic core. The first provides the magnetic field H proportional to its magnetizing current, and the second, realized with thin copper wire wrapped very close to the magnetic core, provides the magnetic flux density B, proportional to the induced voltage.

The test bench realized in own laboratories allows to supply the toroids with compensated waveforms until 2 kHz, providing sinusoidal waveforms with very low harmonic content (Total Harmonic Distortion, THD, lower than 1%). A dedicated data acquisition system prepared with LabView code allows to acquire data calculating the magnetic and energetic properties. The scheme of the acquisition system is reported in Figure 5, while Figure 6 shows an example of the data acquisition and elaboration.

A complete data acquisition can require around 15 min.

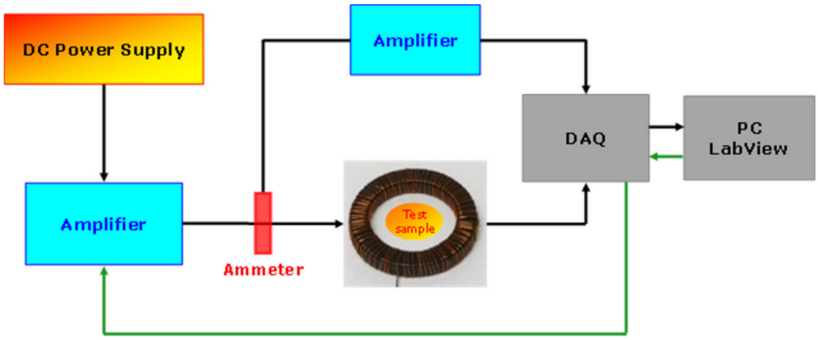

Figure 5. Magnetic characterization system setup with Lab View platform (DAQ—Data Acquisition).

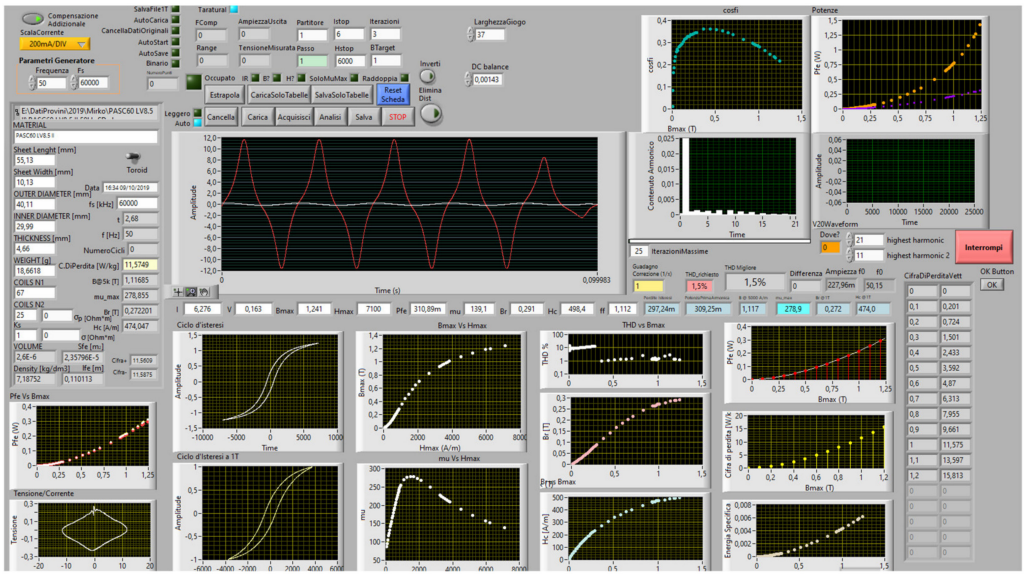

Figure 6. LabView interface with real-time flux waveform control and advanced elaboration of magnetic and losses properties.

3.1. BH Curves

The main output of the magnetic characterization is the trace of the magnetic characteristic of the proposed SMC materials as a function of the temperature. The BH traces are reported hereafter, respectively, E 0.2-500 in Figure 7, E 0.2-700 in Figure 8 and E 0.5-700 in Figure 9. The results confirm that the temperature does not affect the anhysteretic magnetic characteristics. The samples with low binder content and compacted at high pressure show the best BH curves (1.33 T at 5000 A/m), but those results are independent of the temperature during the measurement.

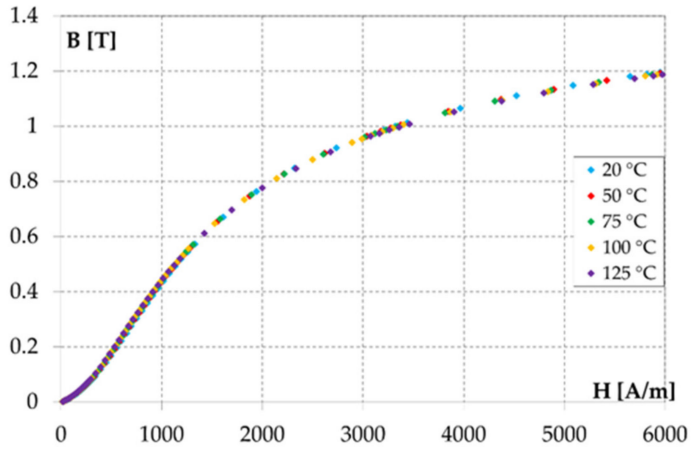

Figure 7. BH curves at different temperatures of SMC sample E 0.2-500.

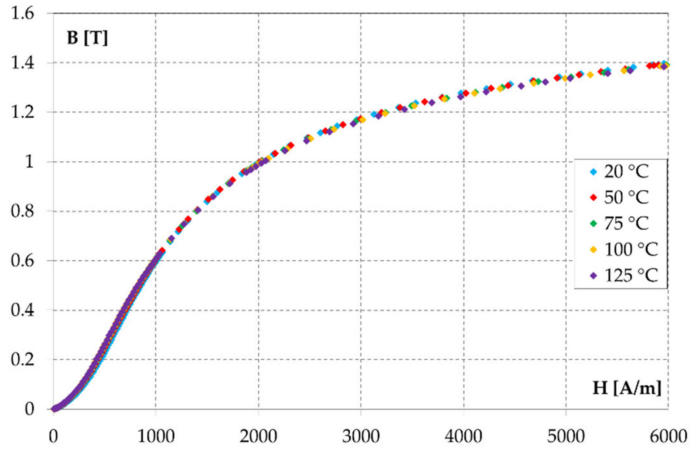

Figure 8. BH curves at different temperatures of SMC sample E 0.2-700.

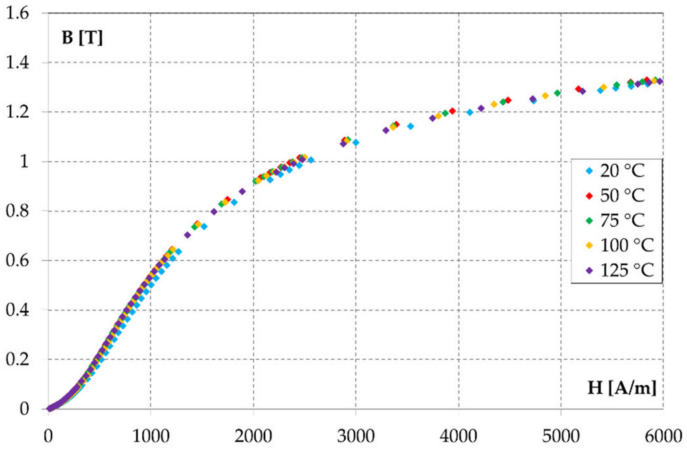

Figure 9. BH curves at different temperatures of SMC sample E 0.5-700.

3.2. Maximum Magnetic Permeability

The measurements of maximum magnetic permeability have been conducted and are shown in Figure 10. The impact of the operating temperature is closely related to the typologies of SMC samples. For E 0.5-700, the temperature effect is negligible, while for SMC materials with lower binder content (E 0.2-500 and E 0.2-700), the maximum magnetic permeability increases with temperature.

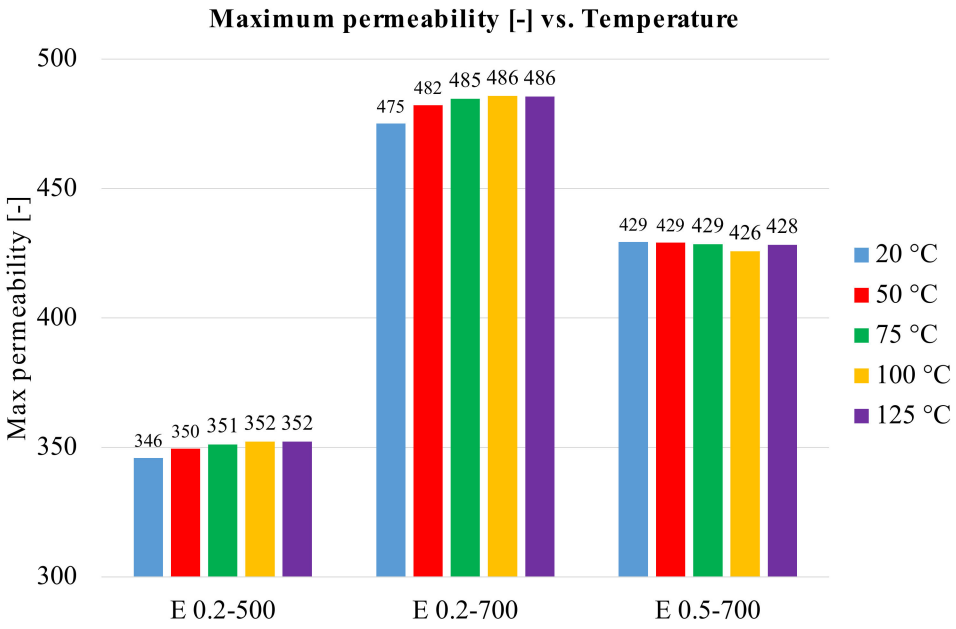

Figure 10. Maximum magnetic permeability of SMC samples for different temperatures.

3.3. Hysteresis Cycles

Further information about the magnetic behavior of the SMC specimens have been obtained by measuring the hysteresis cycles, which are reported in the following Figures 11–13, as a function of the temperature, with the respective reduction of the coercive field H_c, indicated in the lower quadrant of each graph. It can be pointed out that the specimen with higher density, and better hysteresis cycle, presents lower percentage reduction of the coercive field H_c.

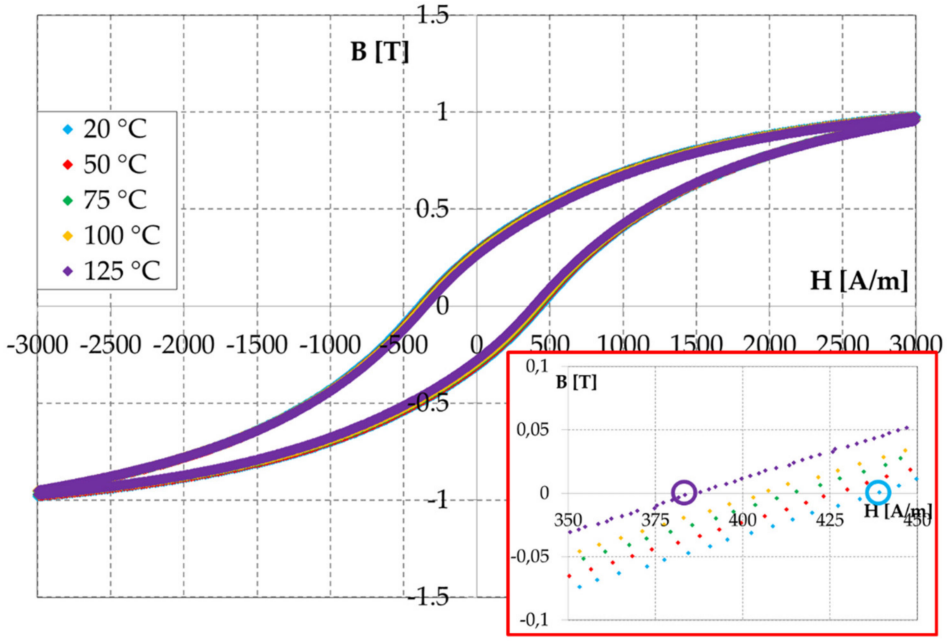

Figure 11. Hysteresis cycles at different temperatures of SMC sample E 0.2-500 for different temperatures.

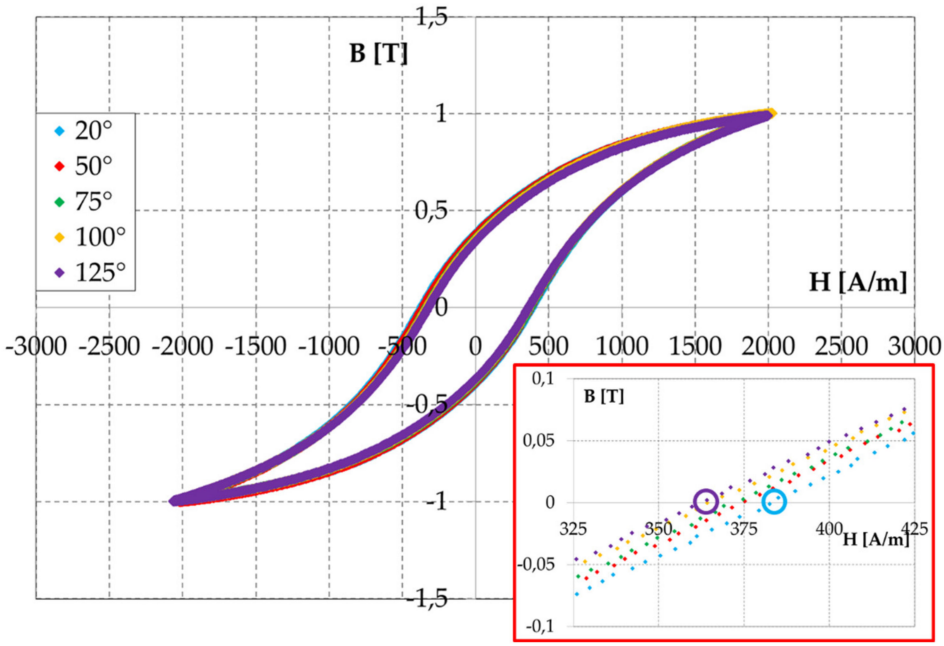

Figure 12. Hysteresis cycles at different temperatures of SMC sample E 0.2-700 for different temperatures.

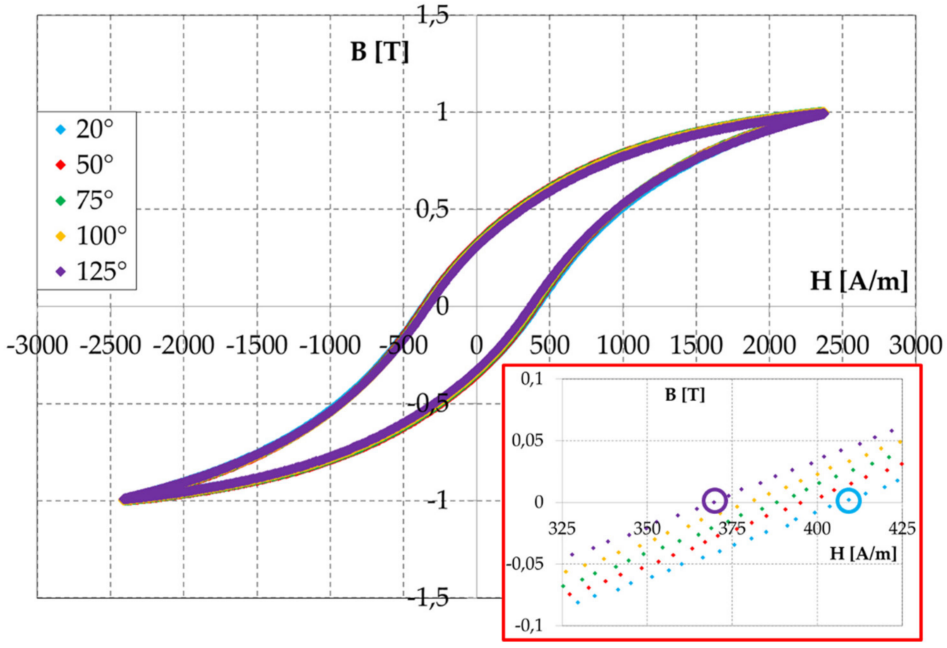

Figure 13. Hysteresis cycles at different temperatures of SMC sample E 0.5-700 for different temperatures.

3.4. Specific Iron Losses

In the case of specific iron losses, the measurements at 1T and 50 Hz have been deduced and are shown in Figure 14. For all the considered specimens, the iron losses present uniform tendency, lowering with the temperature increase. The thermal energy adds to that of the excitation field, making it easier to overcome the pinning sites and, as a consequence, the Block walls move more freely. The temperature effect is not affected by the SMC typologies; just a slight improvement can be observed for samples with low binder content (E 0.2-500 and E 0.2-700) compared to high binder content.

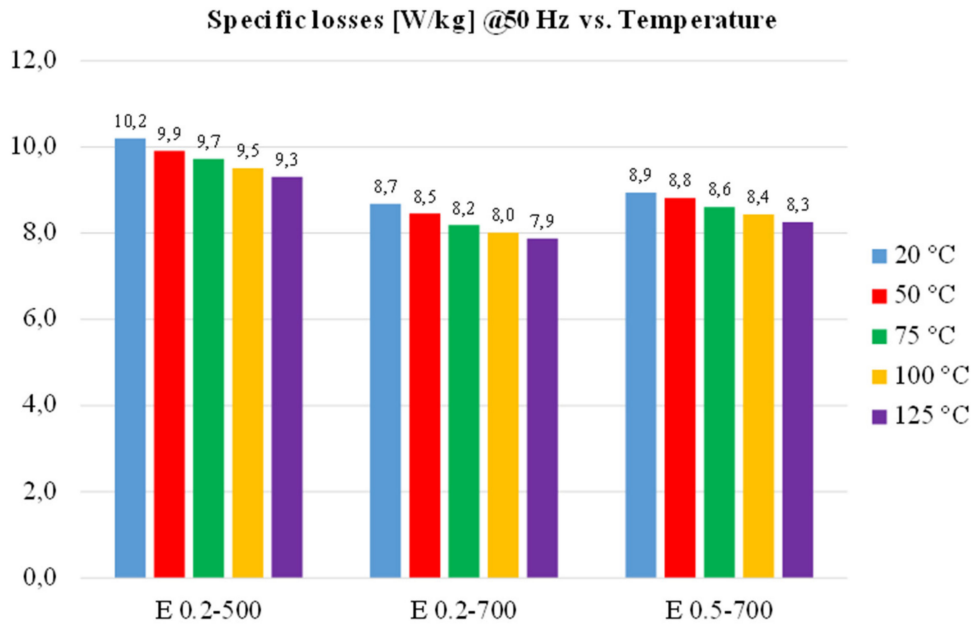

Figure 14. Specific iron losses @1T and 50 Hz at different temperatures of SMC samples.

The tests have also been repeated for different supply frequency levels to investigate its possible impact on the losses; the consequent specific iron losses values are reported in Table 2, as a function of the operating temperature and frequency. From these results, it is possible to deduce the percentage reduction of the iron losses as reported in Table 3.

Table 2. Specific iron losses for different frequencies.

Specimen Typology and Temperature		Specific Iron Losses @ 1T (W/kg) Frequency [Hz] 50	400	500
E 0.2-500	**20 °C**	10.20	107.14	141.56
	125 °C	9.30	99.85	132.39
E 0.2-700	**20 °C**	8.68	89.06	117.37
	125 °C	7.87	80.83	106.60
E 0.5-700	**20 °C**	8.94	93.29	123.01
	125 °C	8.25	86.72	114.30

Table 3. Effect of the operating temperature condition on specific iron losses % reduction (comparison between 20 °C and 125 °C).

Scheme 1. T (%).			
Specimen Typology	**Frequency (Hz)** 50	400	500
E 0.2-500	−9%	−7%	−6%
E 0.2-700	−9%	−9%	−9%
E 0.5-700	−8%	−7%	−7%

The reduction of iron losses may be attributed to the minor hysteresis component of the losses; on the other hand, the presence of excess losses is not negligible in SMC materials [52–56]. Therefore, the correct evolution of different iron losses components with temperature increase requires a detailed analysis.

The magnetic and energetic properties were also checked at 50 °C after having completed the characterization as a function of the temperature, obtaining the same results

previously obtained. Based on our experience of a large variety of materials, stable improvements should be obtained with heat treatments over 200–250 °C.

As the obtained results should be considered of significant interest for what concerns the behavior of the investigated SMC materials with respect to the actual operating temperature, the authors also decided to carry out a similar activity on a laminated steel. A toroidal core was realized with a M400-50A steel (0.5 mm thick) punched in the same size of the SMC specimens (external diameter 40 mm, internal diameter 30 mm, total thickness 5.07 mm), and was tested in the same temperature and frequency conditions.

The test data on the above-mentioned steel are reported in Figure 15 and Table 4, providing the losses variation from 20 °C to 125 °C of operating temperature

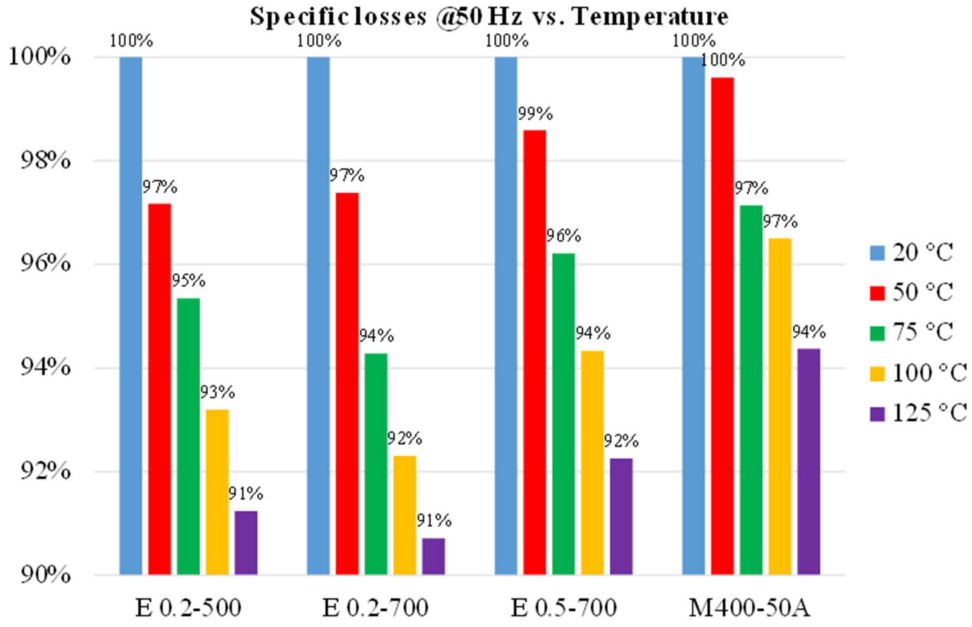

Figure 15. Specific iron losses (@1T and 50 Hz) percentage reduction for SMC samples and laminated steel.

Table 4. Effect of the operating temperature condition on specific iron losses % reduction (comparison between 20 °C and 125 °C) in a laminated steel.

Specific Iron losses @ 1T (%)			
Laminated Steel	**Frequency (Hz)**		
	50	**400**	**500**
M400-50A	−6%	−7%	−7%

4. Conclusions

The effect of the operating temperature on the magnetic and energetic behavior of SMC materials has been experimentally obtained. The results show that the maximum magnetic permeability improves with the temperature increase, and even better results are obtained on the specific iron losses reduction. It is evident that the binder content affects the energetic behavior of SMCs in the expected operating conditions, and the values remain constant at different frequencies. Instead, low pressure levels involve a further slight reduction at high frequencies. Probably, the dependence of the iron losses in the SMC materials at different thermal conditions lies in the hysteresis and excess losses behavior. Under this point of view, a correct separation of iron losses components must be considered mandatory, and this activity will be pursued in the immediate future, together with the mechanical performance behavior in temperature (requiring a specific climatized

instrument), taking under consideration the actual electrical machine operating condition. Finally, other typologies of SMC materials will be tested in future activities.

Author Contributions: Conceptualization, E.P. and L.F.; methodology, F.F.; software, F.F.; validation, L.F., R.B. and M.A.G.; formal analysis, M.A.G.; investigation, E.P.; resources, L.F.; data curation, L.F.; writing—original draft preparation, L.F., E.P.; writing—review and editing, M.A.G., R.B. All authors have read and agreed to the published version of the manuscript.

Funding: This research received no external funding.

Institutional Review Board Statement: Not applicable.

Informed Consent Statement: Not applicable.

Data Availability Statement: Not applicable.

Conflicts of Interest: The authors declare no conflict of interest.

References

1. Bureš, R.; Strečkova, M.; Faberova, M.; Kollar, P.; Fuzer, J. Advances in powder metallurgy soft magnetic composite materials. *Arch. Met. Mater.* **2017**, *62*, 1149–1154. [CrossRef]
2. Sunday, K.J.; Taheri, M.L. Soft magnetic composites: Recent advancements in the technology. *Met. Powder Rep.* **2017**, *72*, 425–429. [CrossRef]
3. Périgo, E.A.; Weidenfeller, B.; Kollár, P.; Füzer, J. Past, present and future of soft magnetic composites. *Appl. Phys. Rev.* **2018**, *5*, 031301. [CrossRef]
4. Zhao, G.; Wu, C.; Yan, M. Enhanced magnetic properties of Fe soft magnetic composites by surface oxidation. *J. Magn. Magn. Mater.* **2016**, *399*, 51–57. [CrossRef]
5. Sunday, K.J.; Hanejko, F.G.; Taheri, M.L. Magnetic and microstructural properties of Fe_3O_4-coated Fe powder soft magnetic composites. *J. Magn. Magn. Mater.* **2017**, *423*, 164–170. [CrossRef]
6. Füzer, J.; Strečková, M.; Dobák, S.; Ďáková, Ľ.; Kollár, P.; Fáberová, M.; Bureš, R.; Osadchuk, Y.; Kurek, P.; Vojtko, M. Innovative ferrite nanofibres reinforced soft magnetic composite with enhanced electrical resistivity. *J. Alloys Compd.* **2018**, *753*, 219–227. [CrossRef]
7. Yaghtin, M.; Taghvaei, A.H.; Hashemi, B.; Janghorban, K. Effect of heat treatment on magnetic properties of iron-based soft magnetic composites with Al_2O_3 insulation coating produced by sol–gel method. *J. Alloys Compd.* **2013**, *581*, 293–297. [CrossRef]
8. Luo, F.; Fan, X.; Luo, Z.; Hu, W.; Wang, J.; Wu, Z.; Li, G.; Li, Y.; Liu, X. Preparation and magnetic properties of FeSiAl-based soft magnetic composites with MnO/Al_2O_3 insulation layer. *J. Magn. Magn. Mater.* **2020**, *498*, 166084. [CrossRef]
9. Bidulský, R.; Bidulská, J.; Grande, M.A.; Ferraris, L. Aluminium alloy addition effects on the behaviour of soft magnetic materials at low frequencies. *Acta Metall. Slovaca* **2014**, *20*, 271–278. [CrossRef]
10. Zhou, B.; Dong, Y.; Liu, L.; Chang, L.; Bi, F.; Wang, X. Enhanced soft magnetic properties of the Fe-based amorphous powder cores with novel TiO_2 insulation coating layer. *J. Magn. Magn. Mater.* **2019**, *474*, 1–8. [CrossRef]
11. Yan, L.; Yan, B. Fe-Si/$MnZn(Fe_2O_4)_2$ Core-shell Composites with Excellent Magnetic Properties by Mechanical Milling and Spark Plasma Sintering (SPS). *Metals* **2018**, *8*, 553. [CrossRef]
12. Wu, Z.; Fan, X.; Wang, J.; Li, G.; Gan, Z.; Zhang, Z. Core loss reduction in Fe–6.5wt.%Si/SiO_2 core–shell composites by ball milling coating and spark plasma sintering. *J. Alloys Compd.* **2014**, *617*, 21–28. [CrossRef]
13. Luo, Z.; Fan, X.; Hu, W.; Luo, F.; Wang, J.; Wu, Z.; Liu, X.; Li, G.; Li, Y. High performance Fe-Si soft magnetic composites coated with novel insulating-magnetic-insulating (IMI) layer. *J. Magn. Magn. Mater.* **2020**, *496*, 165937. [CrossRef]
14. Pošković, E.; Ferraris, L.; Franchini, F.; Bidulsky, R.; Actis Grande, M. Novel SMC Materials with the Insulating Layer Treated at High Temperature. In Proceedings of the EPMA Euro PM2019, Maastricht, The Netherlands, 13–16 October 2019; European Powder Metallurgy Association: Chantilly, France, 2019.
15. Zheng, J.; Zheng, H.; Lei, J.; Qiao, L.; Ying, Y.; Cai, W.; Li, W.; Yu, J.; Liu, Y.; Huang, X.; et al. Structure and magnetic properties of Fe-based soft magnetic composites with an Li–Al–O insulation layer obtained by hydrothermal synthesis. *J. Alloys Compd.* **2020**, *816*, 152617. [CrossRef]
16. Actis Grande, M.; Bidulský, R.; Cavagnino, A.; Ferraris, L.; Ferraris, P. Investigations on different processing conditions on softmagnetic composite material behavior al low frequency. *IEEE Trans. Ind. Appl.* **2012**, *48*, 1335–1343. [CrossRef]
17. Dias, M.M.; Mozetic, H.J.; Barboza, J.S.; Martins, R.M.; Pelegrini, L.; Schaeffer, L. Influence of resin type and content on electrical and magnetic properties of soft magnetic composites (SMCs). *Powder Technol.* **2013**, *237*, 213–220. [CrossRef]
18. Ferraris, L.; Pošković, E.; Franchini, F. New soft magnetic composites for electromagnetic applications with improved mechanical properties. *AIP Adv.* **2016**, *6*, 056209. [CrossRef]
19. Taghvaei, A.H.; Shokrollahi, H.; Janghorban, K. Magnetic and structural properties of iron phosphate–phenolic soft magnetic composites. *J. Magn. Magn. Mater.* **2009**, *321*, 3926–3932. [CrossRef]

20. Streckova, M.; Bures, R.; Faberova, M.; Medvecky, L.; Fuzer, J.; Kollar, P. A comparison of soft magnetic composites designed from different ferromagnetic powders and phenolic resins. *Chin. J. Chem. Eng.* **2015**, *23*, 736–743. [CrossRef]
21. Taghvaei, A.H.; Shokrollahi, H.; Ghaffari, M.; Janghorban, K. Influence of particle size and compaction pressure on the magnetic properties of iron-phenolic soft magnetic composites. *J. Phys. Chem. Solids* **2010**, *71*, 7–11. [CrossRef]
22. Kollár, P.; Birčáková, Z.; Vojtek, V.; Füzer, J.; Bureš, R.; Fáberová, M. Dependence of demagnetizing fields in Fe-based composite materials on magnetic particle size and the resin content. *J. Magn. Magn. Mater.* **2015**, *388*, 76–81. [CrossRef]
23. Luo, D.; Wu, C.; Yan, M. Incorporation of the Fe_3O_4 and SiO_2 nanoparticles in epoxy-modified silicone resin as the coating for soft magnetic composites with enhanced performance. *J. Magn. Magn. Mater.* **2018**, *452*, 5–9. [CrossRef]
24. Birčáková, Z.; Füzer, J.; Kollár, P.; Streckova, M.; Szabó, J.; Bureš, R.; Fáberová, M. Magnetic properties of Fe-based soft magnetic composite with insulation coating by resin bonded Ni-Zn ferrite nanofibres. *J. Magn. Magn. Mater.* **2019**, *485*, 1–7. [CrossRef]
25. Meng, B.; Yang, B.; Zhang, X.; Zhou, B.; Li, X.; Yu, R. Combinatorial surface coating and greatly-improved soft magnetic performance of Fe/Fe_3O_4/resin composites. *Mater. Chem. Phys.* **2020**, *242*, 122478. [CrossRef]
26. Poskovic, E.; Franchini, F.; Grande, M.A.; Ferraris, L.; Bidulsky, R. Innovative Soft Magnetic Composite Materials: Evaluation of magnetic and mechanical properties. *De Gruyter Open Eng.* **2018**, *8*, 368–372. [CrossRef]
27. Zhou, B.; Chi, Q.; Dong, Y.; Liu, L.; Zhang, Y.; Chang, L.; Pan, Y.; He, A.; Li, J.; Wang, X. Effects of annealing on the magnetic properties of Fe-based amorphous powder cores with inorganic-organic hybrid insulating layer. *J. Magn. Magn. Mater.* **2020**, *494*, 165827. [CrossRef]
28. Grande, M.A.; Ferraris, L.; Franchini, F.; Pošković, E. New SMC materials for small electrical machine with very good mechanical properties. *IEEE Trans. On Ind. Appl.* **2018**, *54*, 195–203. [CrossRef]
29. Khan, M.A.; Chen, Y.; Pillay, P. Application of soft magnetic composites to PM wind generator design. In Proceedings of the IEEE Power Engineering Society General Meeting, Montreal, QC, Canada, 18–22 June 2006; pp. 1–4. [CrossRef]
30. Schoppa, A.; Delarbre, P.; Schatz, A. Optimal Use of soft magnetic powder composite (SMC) in Electric Machines. In Proceedings of the MPIF PowderMet, Chicago, IL, USA, 24–27 June 2013; pp. 10-130–10-139.
31. Cros, J.; Perin, A.J.; Viarouge, P. Soft magnetic composites for electromagnetic components in lighting applications. In Proceedings of the IEEE IAS Annual Meeting, Pittsburgh, PA, USA, 13–18 October 2002; pp. 342–347.
32. Ferraris, L.; Poskovic, E.; Franchini, F.; Grande, M.A.; Bianchi, N. New magnetic materials in the electrical machines: Development and applications. In Proceedings of the EPMA EURO PM2017, Milan, Italy, 1–5 October 2017.
33. Kącki, M.; Rylko, M.S.; Hayes, J.G.; Sullivan, C.R. Magnetic material selection for EMI filters. In Proceedings of the IEEE ECCE Conference, Cincinnati, OH, USA, 1–5 October 2017; pp. 2350–2356. [CrossRef]
34. Silveyra, J.M.; Ferrara, E.; Huber, D.L.; Monson, T.C. Soft magnetic materials for a sustainable and electrified world. *Science* **2018**, *362*, 1–9. [CrossRef] [PubMed]
35. Gheiratmand, T.; Hosseini, H.R.M.; Reihani, S.M.S. Iron-borosilicate soft magnetic composites: The correlation between processing parameters and magnetic properties for high frequency applications. *J. Magn. Magn. Mater.* **2017**, *429*, 241–250. [CrossRef]
36. Wu, Z.Y.; Jiang, Z.; Fan, X.A.; Zhou, L.J.; Wang, W.L.; Xu, K. Facile synthesis of Fe-6.5wt%Si/SiO_2 soft magnetic composites as an efficient soft magnetic composite material at medium and high frequencies. *J. Alloys Compd.* **2018**, *742*, 90–98. [CrossRef]
37. Schoppa, A.; Delarbre, P.; Holzmann, E.; Sigl, M. Magnetic properties of soft magnetic powder composites at higher frequencies in comparison with electrical steels. In Proceedings of the IEEE EDPC Conference, Nuremberg, Germany, 29–30 October 2013; pp. 1–5.
38. Liew, G.S.; Ertugrul, N.; Soong, W.L.; Gehlert, D.B. Analysis and Performance Evaluation of an Axial-Field Brushless PM Machine Utilising Soft Magnetic Composites. In Proceedings of the IEEE IEMDC Conference, Antalya, Turkey, 3–5 May 2007; pp. 153–158.
39. Franchini, F.; Poskovic, E.; Ferraris, L.; Cavagnino, A.; Bramerdorfer, G. Application of new magnetic materials for axial flux machine prototypes. In Proceedings of the IEEE IEMDC Conference, Miami, FL, USA, 21–24 May 2017; pp. 1–6.
40. Chang, J.; Lee, J.; Kim, J.; Chung, S.; Kang, D.; Weh, H. Development of Rotating Type Transverse Flux Machine. In Proceedings of the IEEE IEMDC Conference, Antalya, Turkey, 3–5 May 2007; pp. 1090–1095.
41. Zhu, J.G.; Guo, Y.G.; Lin, Z.W.; Li, Y.J.; Huang, Y.K. Development of PM Transverse Flux Motors With Soft Magnetic Composite Cores. *IEEE Trans. Magn.* **2011**, *47*, 4376–4383. [CrossRef]
42. Doering, J.; Steinborn, G.; Hofmann, W. Torque, Power, Losses, and Heat Calculation of a Transverse Flux Reluctance Machine With Soft Magnetic Composite Materials and Disk-Shaped Rotor. *IEEE Trans. On Ind. Appl.* **2015**, *51*, 1494–1504. [CrossRef]
43. Passenbrunner, J.; Andessner, D.; Kobler, R.; Amrhein, W. Modeling, simulation and design of a claw pole machine using soft magnetic composites. In Proceedings of the IEEE VPPC Conference, Chicago, IL, USA, 6–9 September 2011; pp. 1–6.
44. Maurus, Q.; Löffler, C.; Canders, W. New linear drive concepts by taking advantage of Soft Magnetic Composites (SMC). In Proceedings of the IEEE EPE-PEMC Conference, Ohrid, Macedonia, 6–8 September 2010; pp. S3-21–S3-28.
45. Nord, G.; Jansson, P.; Petersen, C.C.; Yamada, T. Vertical electrical motor using soft magnetic composites. In Proceedings of the IEEE IEMDC Conference, San Antonio, TX, USA, 15 May 2005; pp. 373–377.
46. Pošković, E.; Ferraris, L.; Franchini, F.; Cavagnino, A.; Grande, M.A. SMC Materials in Electrical Machine Prototypes. In Proceedings of the IEEE IEMDC Conference, San Diego, CA, USA, 12–15 May 2019; pp. 2042–2047.
47. Fiorillo, F.; Appino, C.; Pasquale, M. Chapter 1—Hysteresis in Magnetic Materials. In *The Science of Hysteresis*; Bertotti, G., Mayergoyz, I., Eds.; Academic Press: Cambridge, MA, USA, 2006; Volume III, pp. 1–190.

48. Bertotti, G.; Fiorillo, F.; Montorsi, A. The role of grain size in the magnetization process of soft magnetic materials. *AIP J. Appl. Phys.* **1990**, *67*, 5574–5576. [CrossRef]
49. Pan, Y.; Peng, J.; Qian, L.; Xiang, Z.; Lu, W. Effects of compaction and heat treatment on the soft magnetic properties of iron-based soft magnetic composites. *Mater. Res. Express* **2020**, *7*, 016115. [CrossRef]
50. Oikonomou, C.; Hryha, E.; Nyborg, L. An XPS investigation on the thermal stability of the insulating surface layer of soft magnetic composite powder. *ECASIA J. Surf. Interface Anal.* **2016**, *48*, 445–450. [CrossRef]
51. Ferraris, L.; Franchini, F.; Poskovic, E. Overview of SMC characterization for their adoption in electromechanical systems. In Proceedings of the 9th International Conference on Magnetism and Metallurgy (WMM 2020), Rome, Italy, 3–5 November 2020; pp. 75–91.
52. Lauda, M.; Füzer, J.; Kollár, P.; Strečková, M.; Bureš, R.; Kováč, J.; Baťková, M.; Baťko, I. Magnetic properties and loss separation in FeSi/$MnZnFe_2O_4$ soft magnetic composites. *J. Magn. Magn. Mater.* **2016**, *411*, 12–17. [CrossRef]
53. Dobák, S.; Füzer, J.; Kollár, P.; Fáberová, M.; Bureš, R. Interplay of domain walls and magnetization rotation on dynamic magnetization process in iron/polymer–matrix soft magnetic composites. *J. Magn. Magn. Mater.* **2017**, *426*, 320–327. [CrossRef]
54. Anhalt, M.; Weidenfeller, B. Dynamic losses in FeSi filled polymer bonded soft magnetic composites. *J. Magn. Magn. Mater.* **2006**, *304*, e549–e551. [CrossRef]
55. Taghvaei, A.H.; Shokrollahi, H.; Janghorban, K.; Abiri, H. Eddy current and total power loss separation in the iron–phosphate–polyepoxy soft magnetic composites. *Mater. Des.* **2009**, *30*, 3989–3995. [CrossRef]
56. De la Barriere, O.; Appino, C.; Fiorillo, F.; Ragusa, C.; Lecrivain, M.; Rocchino, L.; Ahmed, H.B.; Gabsi, M.; Mazaleyrat, F.; LoBue, M. Characterization and Prediction of Magnetic Losses in Soft Magnetic Composites Under Distorted Induction Waveform. *IEEE Trans. Magn.* **2013**, *49*, 1318–1326. [CrossRef]